Chapter 6

Hypertrophic Cardiomyopathy - Impaired sarcomeric motion and contractile dysfunction caused by defective MYBPC3 in hPSC derived cardiomyocytes

Marcelo C. Ribeiro[1], Matthew J. Birket[1], Leon Tertoolen[1], Jantine Monshouwer-Kloots[1], Christine L. Mummery[1] and Robert Passier[1]

[1]Department of Anatomy & Embryology, Leiden University Medical Center, Leiden, The Netherlands.

Manuscript in preparation

Abstract

Hypertrophic Cardiomyopathy (HCM) is a cardiac disease, morphologically characterized by cardiac hypertrophy, fibrosis and impaired heart function. HCM is primarily associated with mutations in sarcomeric proteins. Mutations in sarcomeric Myosin Binding Protein C (MYBPC3) account for approximately 25% of all HCM patients. The majority of mutations in MYBPC3 are nonsense mutations, predicted to produce truncated proteins. However, instead of truncated proteins, lower levels of full-length protein of MYPBC3 are frequently found in heart samples of patients with mutations in MYBPC3, strongly suggesting that haploinsufficiency is responsible for the cardiac disease phenotype. In Chapter 4 we described a contractile defect in human induced pluripotent stem cell derived cardiomyocytes (hiPSC-CM) from HCM patients carrying a MYBPC3 mutation. In this chapter we demonstrate that decreasing the MYBPC3 protein level through short-hairpin RNA knock-down in normal hPSC-CM induces contractile dysfunction similar to the observations on MYBPC3 mutated hiPSC-CM. Additionally, we observed a decrease in diastolic sarcomere length together with a decrease in shortening and elongation amplitude of the sarcomeres of MYBPC3 deficient hPSC-CM. Knock-down of MYBPC3 did not affect calcium handling of hPSC-CMs, but reduced the ATP consumption per contraction cycle. In summary, we successfully developed a human *in vitro* model for cardiac MYBPC3 haploinsufficiency in combination with state of the art biophysical and imaging techniques, which will allow us future investigation of the molecular mechanisms responsible for HCM.

Introduction

Hypertrophic Cardiomyopathy (HCM) is the most common inherited cardiac disease with an estimated prevalence of 1:500 in the general population[1]. HCM is characterized morphologically by thickening of cardiac walls, mainly induced by hypertrophy and disarray of cardiomyocytes as well as cardiac fibrosis, leading to asymmetric ventricular hypertrophy and obstruction of the left ventricular outflow tract[1]. The clinical symptoms are variable among patients, ranging from asymptomatic individuals to patients with chest angina, cardiac dyspnea, atrial fibrillation and sudden cardiac death[1,2]. Several causal mutations for HCM have been identified in genes encoding sarcomeric proteins such as cardiac myosin binding protein C (MYBPC3) (42%), β-myosin heavy chain (40%), troponin T (6.5%), and myosin light chain 2 (<1%), all with an autosomal dominant inheritance[3]. The different mutations found in each protein can be divided into: 1) missense mutations (causing a single amino acid substitution); 2) nonsense mutations (insertion or deletion of a nucleotide, causing a shift of the open reading frame shifts and consequent a premature stop codon; 3) in-frame insertion or deletion of a number of nucleotides[4]. A nonsense mutation generated by a guanine duplication at the nucleotide position 2373 of the myosin binding protein C (MYBPC3) gene is responsible for nearly one fourth of the HCM cases in the Netherlands and is therefore being considered as a Dutch founder mutation[5]. This mutation is predicted to create a premature stop codon and consequently a truncated protein at the C-terminus[6]. However, a truncated MYBPC3 protein has not been found in heart samples derived from these patients, suggesting that the truncated protein is degraded. A decrease in total amount of MYBPC3 was also found in these patients compelling the thought of a disease-causing haploinsufficiency[6,7].

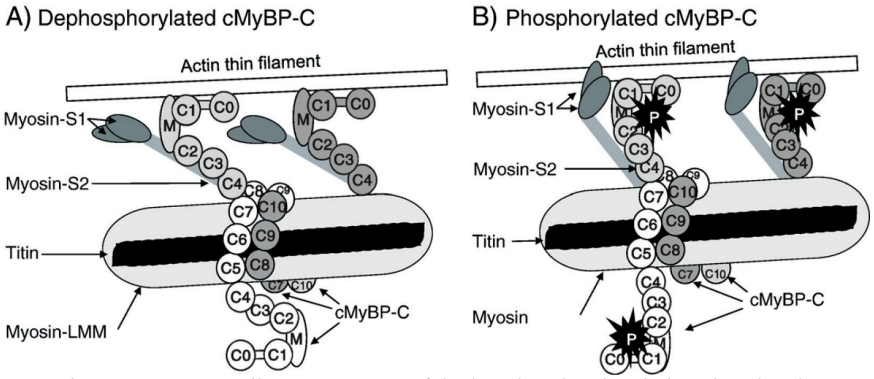

Figure 1- Schematic trimeric collar organization of dephosphorylated and phosphorylated MYBPC3 in the sarcomere. The C5–C10 domains of three MYBPC3 molecules (white, light gray and dark gray) are wrapped around the filament of light meromyosin (myosin-LMM, in light gray) and titin (in black). The overlapping is stabilized by interactions between domains C5:C8 and C7:C10 of two adjacent MYBPC3 molecules. The C0–C4 domains of MYBPC3 are extended into the interfilament space. **A.** when MYBPC3 is dephosphorylated in the MyBP-C motif (M), the C1–M–C2 domains are tightly bound to myosin-S2 (gray rectangles) and actin (white rectangle); this prevents cross-bridges formation. **B.** when MYBPC3 is phosphorylated, M domain releases its interaction with myosin-S2 and actin. This allows myosin heads (myosin-S1) to get ordered and extended to the thin filaments, which results in strong actin–myosin interactions. In contrast to the M domain, C1 domain binds to actin irrespective of the phosphorylation state of MYBPC3 (Taken from Schlossarek S. et. al 2011 with permition).

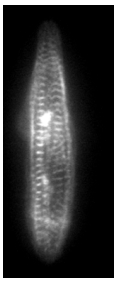

The MYBPC3 is a 140kDa protein, localized transversally in the A-band of cardiac sarcomeres. This protein comprises 11 domains (C0-C10) that connect the thin (actin) to the thick filaments (myosin) through binding of the C0 and C1 domains to the actin filament and C5 to C10 domains to the myosin, titin and light meromyosin (LMM)[4]. Moreover, the C2 to C4 domains together with the MYBPC motif have an important role in modulating contraction as they are tightly bound to the myosin head, preventing its cross-bridge binding the actin during the relaxed state. The MYBPC motif contains three phosphorylation sites that are phosphorylated upon contraction, releasing the interaction with myosin-S2 (**Figure 1**) This release allows the myosin heads to extend and strongly interact with the actin on the thin filament[4]. Even though sarcomeric organization has been well described, the precise function of MYBPC3 during contraction is still not completely understood and direct consequences of various mutations or change in levels of expression have been subject of intensive research. The absence of MYBPC enables the movement of the myosin heads closer to the actin filament[8], increasing the probability of the myosin head being weakly bound to the actin at any given contraction stage. These random cross bridge have been shown to impair the full relaxation of the sarcomere[9] and decrease the strong myosin-actin interactions and force generation during contraction[10]. Random cross bridges not only impair the generation of contractile force but also use energy that is not converted into contraction, which translates to a decreased cardiac output while consuming the same amount of energy. Patients who carry a MYBPC3 mutation display reduced myocardial work relative to oxygen consumption[11]. The impairment of myocardial work indicates that the link between sarcomere mutations and the development of HCM may be related to bioenergetics demand. Further research is needed to fully verify and understand the mechanisms of this disease. Since patient-derived cardiac samples are extremely difficult to obtain and controlled experimental design using primary cardiomyocyte cultures are hampered by the inability to proliferate and the challenging task to maintain viable functional cardiomyocytes *in vitro*. The use of patient-derived induced pluripotent stem cells (iPSC) provides an excellent opportunity to study this. In chapter 4 we showed that cardiomyocytes derived from hiPSC (hiPSC-CM) of patients carrying the 2373dupG mutation display decrease contraction stress when compared to cardiomyocytes derived from hiPSC of healthy donors. In order to have a better understanding of the underlying working mechanism of the disease we established an isogenic human *in vitro* model of MYBPC3 haploinsufficiency using short-hairpin RNAs (shRNAs). Using a multiplex platform we analyzed changes in calcium, sarcomere and contraction kinetics as well as energy consumption caused by the MYBPC3 knockdown in single cardiomyocytes.

Materials and methods

hESC culture and differentiation

The previously described cardiac reporter NKX2-5eGFP/w hESC line[12], was maintained on mouse embryonic fibroblasts (MEFs) and passaged using TrypLE select (Life Technologies). Cardiac differentiation was induced from monolayer cultures on Matrigel in

a serum-free medium (BSA, polyvinyl alcohol, essential lipids [BPEL]) as previously described[13]. The following factors were present for the first 3 days 20 ng/ml BMP4 (R&D), 20 ng/ml Activin A (Miltenyi Biotech) and 1.5 μM CHIR 99021 (Axon Medchem). 5 μM XAV 939 (Tocris Bioscience) was present on days 3-6. Beating cardiomyocyte cultures were dissociated on day 13 and replated on Matrigel-coated 24-well plates. At day 16 cardiomyocyte cultures were refreshed in defined cardiomyocyte culture medium (CCM), which is composed of the following: DMEM (Sigma D5030), 15 mM glucose, 0.5 mM sodium pyruvate, 0.19 mM sodium hydroxybutyrate, 0.5 mM L-carnitine, 1 mM creatine, 5 mM taurine, phenol red (0.011 g/l), 1x Trace elements (A, B and C; Corning), 1x chemically defined lipids (Life Technologies), 2 mM Glutamax, 400 μM α-thioglycerol, 0.1x ITS-X, 50 μg/ml AA-2P, 0.5% Pen-Strep, 3.5 g/l sodium bicarbonate, 100 nM T3, 100 ng/ml Long R3 IGF-1 and 1 μM dexamethasone (TID).

Lentiviral transduction

shRNAs against MYBPC3 (NM_000256) were obtained from Open Biosystems in the pLKO Puro vector (#1 - TRCN0000082906 (AGCCAGAATATGGTTGGCTTT) and #2 - TRCN0000082903 (CCTCCCTACTGTTGGATGTAT). A scrambled control shRNA was used as control (Sarbassov et al., 2005) (Addgene plasmid: 1864). The lentivirus containing pLenti CMV Puro DEST α-actinin-mCherry was described in chapter 5. Cardiomyocytes were transduced with lentiviruses on day 15 of differentiation and subsequently selected with puromycin before single cell dissociation and analysis.

Western blotting

Samples were lysed with ice cold ELB (50mM HEPES pH 7.0; 250mM NaCl; 5mM EDTA; 0.1% NP-40) with 1:100 Protease Inhibitor Cocktail (Sigma-Aldrich) for 30 mins on ice. The samples were centrifuged at 7,000g for 10 mins and supernatant was quantified for protein content using the Bio-Rad Protein Assay (based on the Bradford dye-binding method). 100μg of the hiPSC-CM lysates were run on a 6% polyacrylamide gel and 30μg of the hESC-CM with the shRNA lysates were run on a 10% polyacrylamide gel together with the protein ladder (Precision Plus Protein dual colour – Bio-Rad). Proteins were transferred to an Amersham Hybond membrane (GE Heathcare- Life Sciences) overnight. The membrane was blocked with blocking buffer (2% milk in PBS) and MYBPC3 protein was detected using a specific antibody: Rabbit IgG anti- MYBPC3 (1:2000) overnight at 4C kindly provided by Dr. Sakthivel Sadayappan (Department of Cell and Molecular Physiology, Health Sciences Division, Loyola University Chicago), followed by incubation with a Horse anti-Rabbit IgG – HRP (1:2000) (Cell Signaling). As an internal control for protein levels, and more specifically cardiomyocytes, we used a mouse IgG anti-Actin (1:1000) (MAB1501 – Millipore) and mouse IgG anti-α-actinin (A7811-Sigma-Aldrich) overnight at 4C, respectively. As a second antibody we used a goat anti-mouse IgG-HRP (1:2000) (Cell Signaling).

Contraction stress, sarcomere dynamics and calcium transients measurements on single cardiomyocytes

Contraction stress

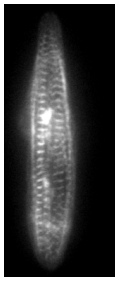

As described in chapter 2 cells were seeded onto gelatine patterned acrylamide gels 4 days before measurements at 37°C and 5% CO2. Briefly, using a Leica AF-6000LX microscope, image-series of aligned single contracting cardiomyocytes paced at 1Hz were taken at a 40x magnification at 20 frames per second, recording brightfield and fluorescent beads (660/680nm). Single frames from maximal relaxation and contraction of the brightfield and fluorescent beads image-series were analyzed by the LIBTRC software package (kindly provided by Dr. Micah Dembo), creating a mask of the cell outline from the brightfield image and a vector map from the difference between the relaxed and contracted fluorescent beads images. The vector map and the cell mask were used to calculate the total force that the cell applies on the substrate at its maximum peak of contraction. The contraction stress generated by the cardiomyocyte during contraction was calculated by dividing the total force by the cell surface area.

Sarcomere dynamics

Contraction cycles of cardiomyocytes were recorded in image series of 500x500 pixels using a 40x dry objective with an internal 1.6x magnification displaying clearly visible and measurable α-actinin-mCherry (587/610nm) expression during at least 6 contractions with a time resolution of 17 milliseconds (56 frames/second). After export to uncompressed TIF format, Image stacks were constructed with the program of ImageJ or Fiji (National Institute of Health NIH U.S.A). The intrinsic function Z-profile of the program was used to construct a line-profile exactly perpendicular to the sarcomeres over the length of one cardiomyocyte. A plugin for ImageJ was written to export the profiles to a time-Z data set. A second program was developed for the interactive analysis using LabVIEW (National Instruments Corporation Austin, U.S.A.) - Power Spectral Analysis. A power spectral analysis per frame (Z-profile) was computed using an Hanning window output. Visual inspection of the power spectra always revealed a single peak and its successive second harmonics. The individual power spectral profiles were then fitted according a Gaussian function using the Levenberg–Marquardt algorithm with a ten times increased time resolution. The center frequency of this fitting (first peak in the spectrum) was used to compute the actual spacing (1/frequency) between the sarcomeres. Finally, all computed points were plotted against time. From this graph, the speed of contraction and relaxation, the contraction duration and the repetition frequency was extracted.

Calcium transients

After recording images for contraction stress and sarcomere dynamics cells were incubated in 5μM of Fluo-4 AM (Invitrogen), unless mentioned otherwise, for 20mins at 37°C and 5%CO2. The change in Fluo-4 intensity (485/520nm) was recorded for each contracting cardiomyocytes paced at 1Hz with a time resolution of 17 milliseconds (56 frames/second) for at least 6 full contractions. Transient recordings were analysed using ImageJ-Fiji in combination with a custom-made software generated to convert raw data to dF/F0 results. The calcium transient duration (from peak amplitude until 90% return to base level, CaT90), amplitude, slope and decay were determined. The time constant of calcium transient decay (τ) was obtained by fitting the decay phase with a single exponential function (y=A0+A1ex-

p[-t/τ]).

Respiration measurements with the Seahorse XF-24 Analyzer

GFP+ cardiomyocytes were sorted by FACS and seeded on Matrigel-coated assay plates at a density of 7x104 cells per well of a Seahorse XF plate, 7 days before measurement. At the time of seeding cells were transduced with lentivirus expressing the scrambled shRNA or the B7 MYBPC3 shRNA. Measurements were performed in bicarbonate-free DMEM (D5030; Sigma Aldrich), containing 0.25% fatty acid-free BovoStar (Bovogen, Australia), 15 mM glucose, 0.5 mM sodium pyruvate, 1 mM sodium lactate, 0.15 mM sodium hydroxybutyrate, 2 mM GlutaMAX (Life Technologies) and 0.5 mM L-carnitine. Cells were washed twice and pre-incubated in assay medium 1 h before measurement. Contraction frequencies of each well were recorded manually at 37°C just before measurement. To assess ATP demand for contraction, after recording the basal respiration rate 5 μg/ml blebbistatin was injected and the respiration rate immediately recorded, followed by measurements after injection of oligomycin to inhibit ATP synthase and then rotenone and antimycin A to interfere with the electron transport chain. A vehicle-only injection was performed in parallel for normalization. In addition, a standard protein assay was used to normalize values to whole cell protein. The oligomycin-sensitive oxygen consumption was converted to an ATP production rate using a P/O ratio of 2.3 as previously described [14].

Statistical analysis

Differences between the different groups were assessed by Student's t-test for comparison of two groups or one-way ANOVA followed by Bonferroni post-test for comparison of three or more groups. The differences in cell structure classification were assessed using Chi2 test.

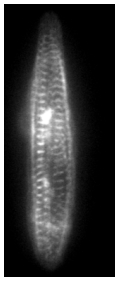

Results

In chapter 4 we described an *in vitro* model that effectively mimics the contractile dysfunction observed in patients. However, this model was based on hiPSC-CM derived from different individuals with different genetic background. In order to minimize the phenotypical differences due to genetic background, we decreased MYBPC protein levels by shRNAs knock down in single hESC lines.

Two different shRNAs specifically targeting MYBPC3 and one scrambled were delivered by lentiviral transduction into cardiomyocytes differentiated form the Hes3-NKX2-5eGFP/w hESC line. Both shRNA constructs effectively decreased mRNA levels and protein expression of MYBPC3 in these cells, when normalized for the effects of control scrambled shRNA (**Figure 2A, B** and **C**). Further experiments were performed in a cardiomyocyte culture medium (CCM) containing TID with entirely defined basal components and no serum albumin (see Experimental procedures) to maximize functional output. In order to analyse changes in the sarcomere dynamics, hESC-CM were co-transduced with a lentivirus carrying the α-actinin-mCherry as described in chapter 5. The cells were cultured for 10 days after virus transduction in CCM before seeding on the patterned lines for contraction stress

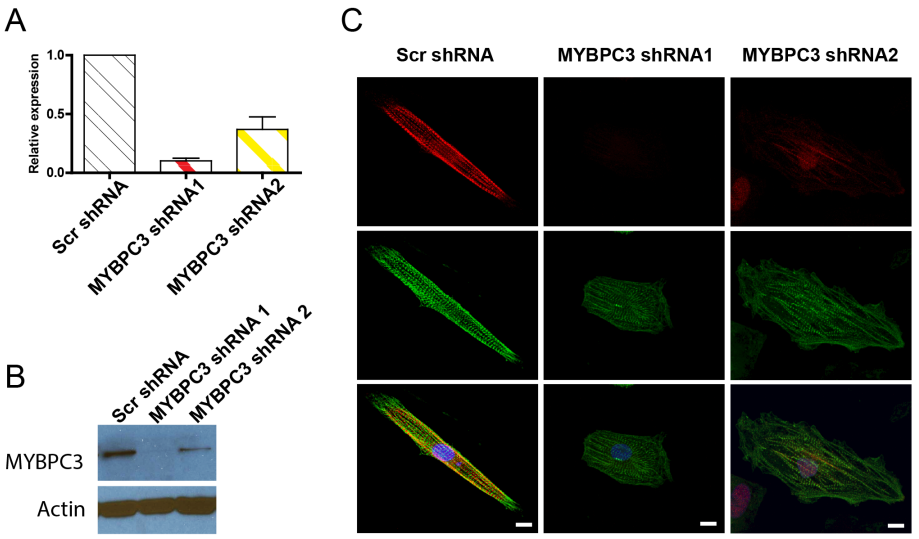

Figure 2- Knocking down MYBPC3 in hESC-CM. **A.** Relative MYBPC3 mRNA expression in hESC-CM transfected with scrambled (SCR) shRNA or two distinct MYBPC3 shRNA (N=3). Expression levels were normalized to RPLP expression. **B.** Western blot assessment of MYBPC3 protein expression after knockdown. C. Sarcomeric immunostaining on hESC-CM after MYBPC3 knockdown; Red-MYBPC3; Green-Troponin I; Blue-Nucleus.

measurements. Since the contraction force setup is based on optical recordings at excitation/emission 660/680nm, additional measurements can be recorded at other wavelengths, such as sarcomere dynamics at 587/610nm and calcium kinetics at 485/520nm on the same cardiomyocytes (**Figure 3**).

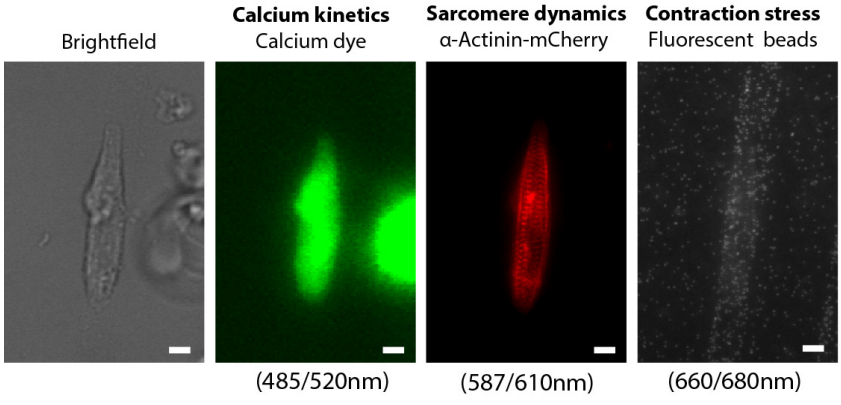

Figure 3 – Example of the single cell multiplex platform. Grey left- Brightfield picture of a beating cardiomyocytes. Green middle- Single frame of calcium transients measurements using Fluo-4; Red middle- α-Actinin-mCherry used to analyse sarcomere dynamics; B&W right- Fluorescent beads embedded on the polyacrylamide gel for contraction stress measurements.

Knocking down MYBPC3 (shRNA) induced a significant decrease in contraction stress of hESC-CM but no changes in cell size were observed (**Figure 4A** and **B**), which is consistent with our previous findings using hiPSC-CM from patients with the c.2373dupG mutation, as described in chapter 4. This suggest that contractile defects are indeed due to haploinsufficiency for MYBPC3. To determine whether the decrease in contraction stress was caused by changes in sarcomere dynamics, movement of α-actinin-mCherry positive Z-disks during contraction were recorded on the same cardiomyocytes. Although the majority of the cardiomyocytes were transduced, only the minority of cardiomyocytes assembled α-actinin-mCherry to a level that is clearly visible and measurable (Chapter 5). Preliminary data showed that the shRNA induced a significant reduction in the diastolic sarcomere length together with a decrease in shortening and elongation amplitude (average distance migrated by each sarcomere during contraction and relaxation, respectively) (**Figure 5A**, **B** and **C**). Additionally, there is a trend in the decrease of the shortening and elongation speeds of sarcomeres in the shRNA cardiomyocytes (**Figure 5D** and **E**), suggesting both impaired relaxation and contraction of the sarcomeres. Additional experiments need to be performed in order to analyse the relation between sarcomere dynamics and contractile force generation for each group. Nevertheless, if both shRNA and Scr groups are combined there is a correlation between force generation of individual cardiomyocytes and the amplitude of sarcomere shortening, amplitude of sarcomere relaxation as well as with the sarcomere diastolic length. However, this correlation does not exist between force generation and systolic length (**Figure 6 A, B, C** and **D**).

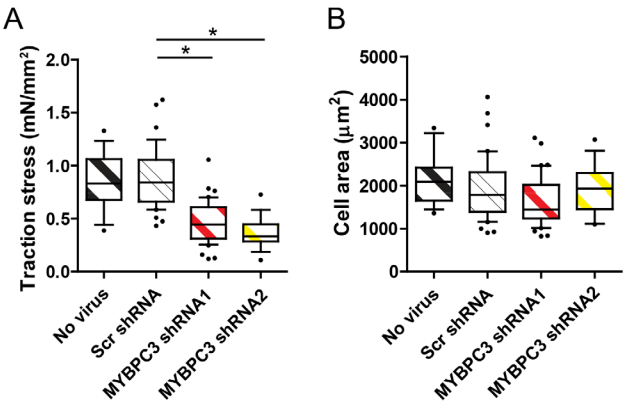

Figure 4- Contractile force changes of cardiomyocytes with MYBPC3 knockdown **A.** Contraction stress and **B.** cell size measured on single hESC-CM with no virus (n=15) or transduced with a scrambler (n=32) or two different MYBPC3 shRNA (n=26 and 16); . *P<0.05.

Several studies have described changes in calcium handling as an important characteristic of hypertrophic cardiomyocytes[9,15–17]. Therefore, assessing the impact of MYBPC3 knock down on calcium handling properties may shed some light on the HCM disease state of this human *in vitro* model. After contraction stress measurements, the cardiomyocytes were loaded with 5µM Fluo-4 for 20mins and the fluorescence intensity change was recorded in each contracting cardiomyocyte. To control for the effect of the calcium buffering by the Fluo-4 each cardiomyocyte was measured again for contraction stress after Fluo-4 load-

ing. No changes in any calcium kinetics parameters were observed on the shRNA treated cardiomyocytes in comparison with the controls (**Figure 7A, B, C, D** and **E**). Nevertheless, the effect of calcium buffering of the Fluo-4 on the single cardiomyocytes greatly affected the contraction stress generation of the cardiomyocytes from all groups (**Figure 7F**), indicating that the high concentration of dye was compromising the contractile machinery of the cardiomyocytes.

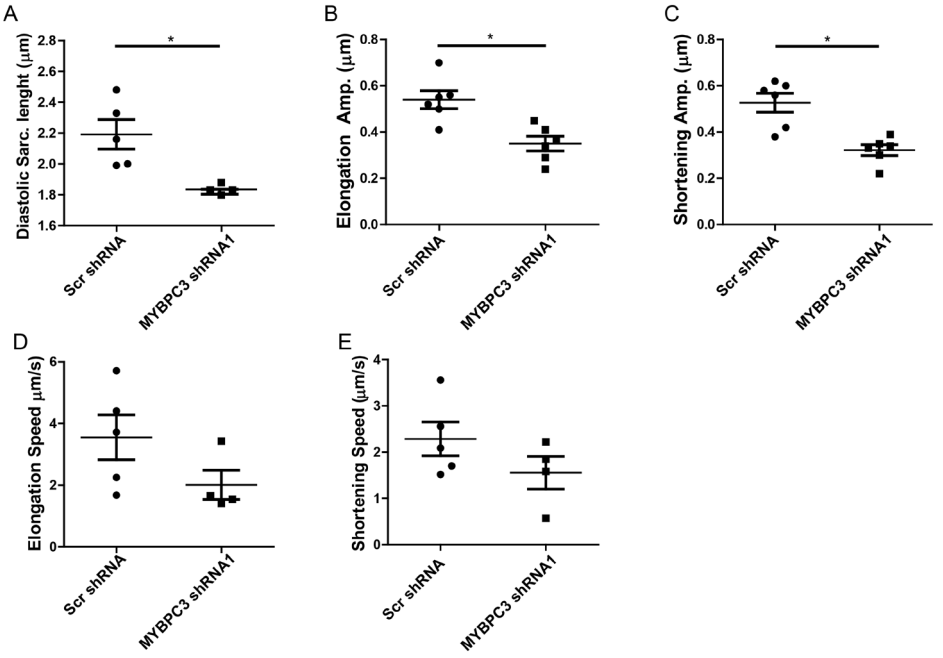

Figure 5- Changes in sarcomere dynamics of cardiomyocytes with MYBPC3 knockdown. **A.** Sarcomere length at relaxed state. **B**. and **C.** Average distance migrated by one sarcomere during relaxation and during contraction, respectively. **D.** and **E.** Average speed at which one sarcomere moves during relaxation and contraction, respectively (Scr n=6; MYBPC3 shRNa1 n=6). *P<0.05.

Recent studies suggested that MYBPC3 deficiency may give rise to HCM because of an increased energy requirement for muscle contraction[11,18]. To test this, bioenergetic profiles of contracting cardiomyocyte monolayers were determined using the Seahorse XF24 Analyzer on cardiomyocytes from the same experimental groups. Contraction rates, measured prior to analysis, were not significantly different between groups. Under standard conditions (15 mM glucose, 0.5 mM sodium pyruvate) normalized to total cell protein, the basal respiration rate and the ATP turnover appeared slightly but not significantly decreased in cardiomyocytes transduced with MYBPC3 shRNA (**Figure 8A, B** and **C**). Moreover, blebbistatin-sensitive respiration rate per contraction cycle was decreased significantly, which is translated to a reduction of ATP use by the actomyosin ATPase for each contraction cycle (**Figure 8D**).

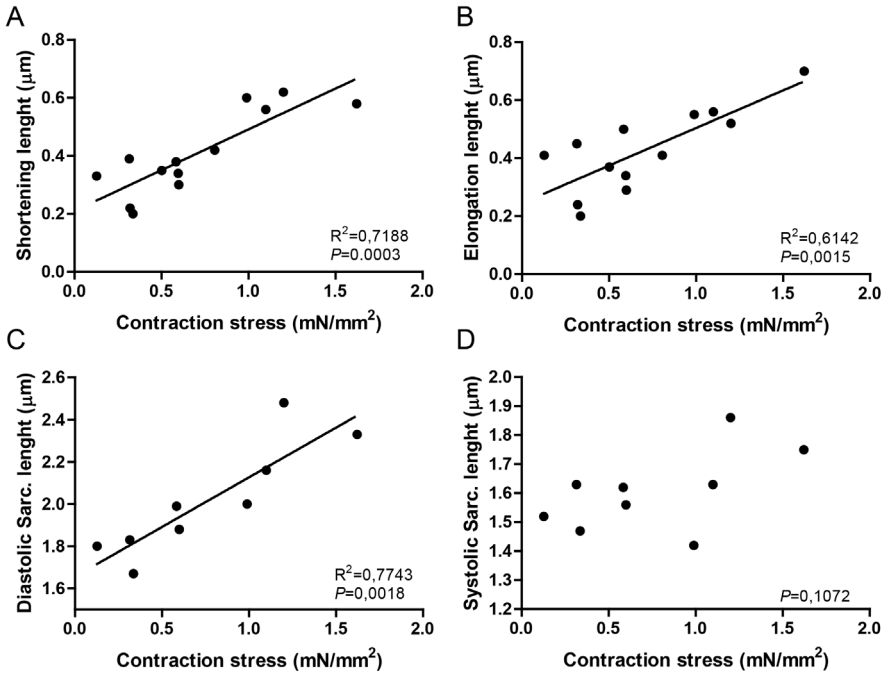

Figure 6- Relation between total contraction stress and sarcomere dynamics. **A.** and **B.** Correlation between contraction stress and average distance migrated by one sarcomere during relaxation or during contraction, respectively. **C.** Correlation between contraction stress and sarcomere length at relaxed state. **D.** Contraction stress does not correlate with sarcomere length at contracted state. With P<0.05* and P<0.01** a correlation was considered existent and a linear regression line was drawn (black line) with the respective R2; With P >0.05 no correlation was considered existent and therefore no linear regression line was drawn.

Discussion

In the work described we developed a human stem cell derived model for multiplex analysis of cardiomyocyte function in disease-simulating conditions. Knockdown of MYBPC3, which mimics the reduced levels of MYBPC3 in HCM patients, resulted in contractile impairment, defects in sarcomeric relaxation and contractile properties and a decrease in bioenergetic demand in hESC-derived cardiomyocytes. We combined different tools developed in previous chapters creating a multiplex platform for measuring contraction stress, sarcomere dynamics and calcium transients in individual cells.

This was a follow up study to chapter 4 where we demonstrated impaired contractile stress in patient derived hiPSC-CM with mutations in MYBPC3. Although the effects on contractile stress were evident, it was unclear whether reduced levels of MYBPC3 were sufficient for the cause of the observed phenotype. Furthermore, we also investigated in more detail the underlying mechanism, by measuring various functional assays in control and diseased cardiomyocytes. For this we knocked down MYBPC3 protein in hESC-CM, enabling us to study the specific role of this protein in cardiomyocyte function by comparing isogenic hESC-CMs with and without knockdown. Alternatively, to determine the causal relation-

ship between the affected protein and the disease phenotype, diseased hiPSC bearing the mutation could be genetically rescued by correcting the mutation, creating an isogenic control. It has been shown previously that the 2373dupG mutation resulted in a decrease of MYBPC3 protein levels human myectomy samples[7], suggesting that the disease is caused by haploinsufficiency of MYBPC3. The contractile defect observed in the cardiomyocytes with decreased MYBPC3 content is consistent with the phenotype observed in patients' cardiac samples[11]. Although the contractile force measurement is a direct consequence of sarcomeric function, a correlation has not been previously shown in hPSC-CM models. The shorter diastolic sarcomeric length and the impairment of shortening and lengthening amplitudes caused by the reduction of MYBPC3 is congruent with previously reported findings in mouse models[9], which substantiates the notion that this protein plays a crucial role in sarcomere function and stability. Moreover, the positive correlation observed between these parameters of sarcomere dynamics and the total contractile force suggests that reduction of MYBPC3 levels impairs contraction stress by disrupting sarcomere function. Furthermore, it would be interesting to determine differences in the relationship between contraction stress and sarcomere dynamics in the diseased model versus control. For this we would need to increase the number of samples in order to make robust conclusions.

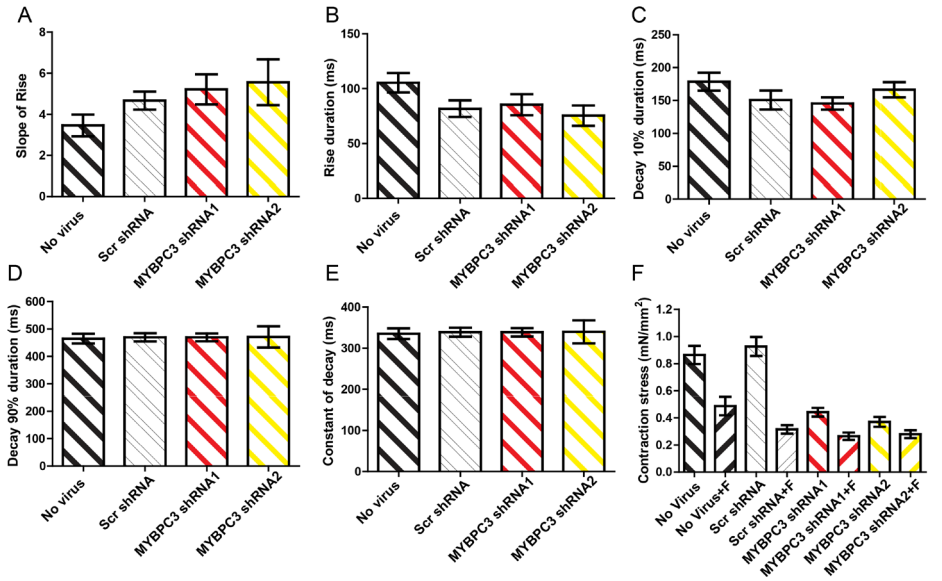

Figure 7- Changes in calcium handling of cardiomyocytes with MYBPC3 knockdown. **A.** and **B.** Slope and duration of rise in intracellular calcium, respectively. **C.**, **D.** and **E.** 10%, 90% and decay constant of intracellular calcium, respectively. **F.** Contraction stress of the same cardiomyocytes before and after (+F) Fluo-4 incubation of each group. No virus-n=10; Scr-n=17; MYBPC3shRNA1-n=16; MYBPC3shRNA2-n=8.

Most individuals carrying a MYBPC3 ultimately develop HCM. Recent studies using patient derived hPSC-CM models of HCM have described this disease phenotype *in vitro* as increased cell size and calcium handling defects[15,17]. However, in our model none of these characteristics are observed in the MYBPC3 deficient cardiomyocytes, which may

indicate that sarcomeric and contractile dysfunction precede an adaptive hypertrophic response. This notion is supported by the fact that HCM is mostly observed later in life of MYBPC3 mutation carriers[11]. It is important to note that the calcium dye evidently affects the excitation-contraction coupling of single cardiomyocytes by buffering the calcium. These observations are reason for concern that Fluo-4 interferes with the calcium handling kinetics: this could be responsible for masking possible differences between disease and control previously described in other HCM causing mutations[15]. The use of calcium dyes has been well established for multicellular platforms in which calcium chelation does not affect the contractile output[19]. On the other hand, single cardiomyocytes are more sensitive to the accumulation of calcium dye inside the cell, which can easily disturb the calcium handling kinetics.

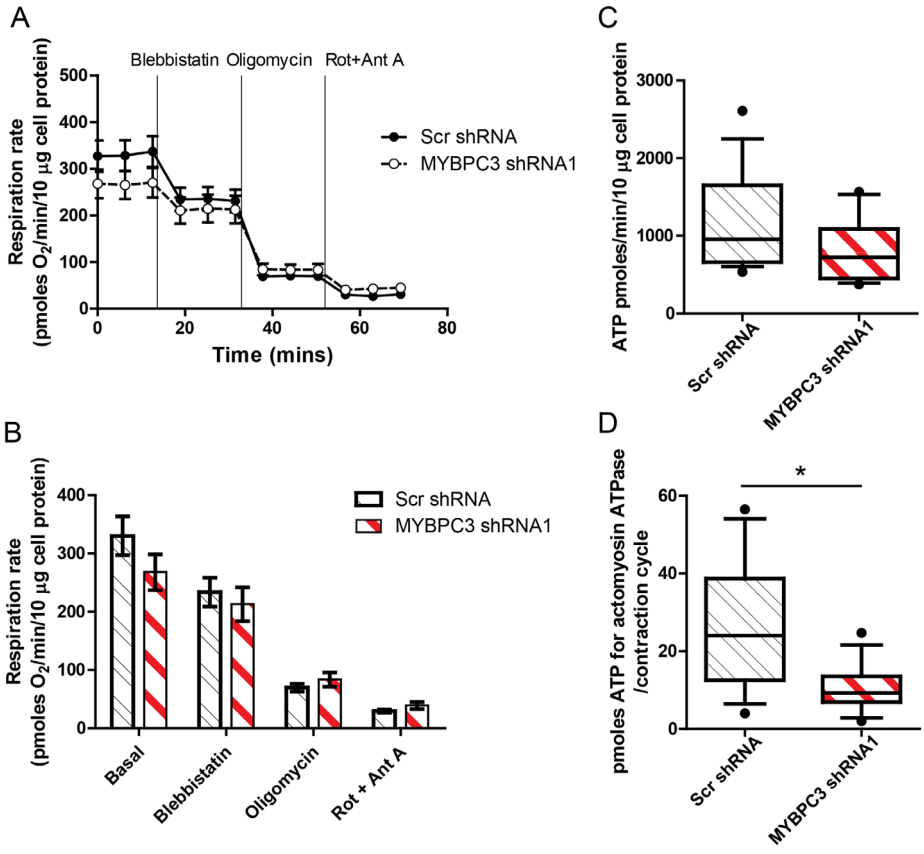

Figure 8- Energy demand for contraction in cardiomyocytes with MYBPC3 knockdown. **A.** Real-time respiration measurements and response to injection of blebbistatin, then oligomycin, and finally rotenone and antimycin A. **B.** Summary data of respiration rates measured at basal activity or in the presence of the factors indicated. **C.** Theoretical ATP production rates from oxidative phosphorylation calculated from the values in **B. D**. Theoretical ATP used by the actomyosin ATPase per contraction cycle. Data in **A** and **B** show mean±sem. The box and whisker plots in **C** and **D** show the median, interquartile range and 10-90 percentile range. n=12-18 measurements acquired over 3 independent experiments. Statistical significance was calculated with an unpaired t-test in **B**, **C** and **D** comparing the scrambled versus the MYBPCshRNA1 rates. *p<0.05.

The knockdown of MYBPC3 induced a decrease of about 50% in the energy usage per contraction cycle, matching the decrease in contractile force generation, meaning that there is similar energy usage per contraction cycle (contractile work) between control and disease groups. This result is not congruent with the theory of increased energy costs per contraction observed in human cardiac samples[11]. One possible explanation for this could be the immature contractile machinery of the hPSC-CM, which might become less function in the absence of MYBPC3 and therefore use less energy.

Conclusion

In this chapter we developed a new disease model for MYBPC3 deficiency using hPSC-derived cardiomyocytes. Knocking down the MYBPC3 in these human cardiomyocytes induced a reduction in contractile force generation, which was correlated with specific changes in sarcomere dynamics. The reduction of MYBPC3 did not affect the calcium handling properties but diminished the energy used per contraction cycle. In conclusion, by applying different tools developed in previous chapters we were able to create a multiplex platform for measuring cardiomyocyte function in individual cells enabling the development of an *in vitro* hPSC-derived disease model for MYBPC3 that recapitulates important functional characteristics of the disease as observed in HCM patients with mutations for MYBPC3, making it a step forward towards studying and understanding the mechanism of cardiomyopathies.

References

[1] [1] Maron BJ, Olivotto I, Bellone P, Conte MR, Cecchi F, Flygenring BP, et al. Clinical profile of stroke in 900 patients with hypertrophic cardiomyopathy. J Am Coll Cardiol. 2002;39(2):301–7.

[2] Maron BJ, Maron MS. Hypertrophic cardiomyopathy. Lancet. 381(9862):242–55.

[3] Richard P, Charron P, Carrier L, Ledeuil C, Cheav T, Pichereau C, et al. Hypertrophic cardiomyopathy: distribution of disease genes, spectrum of mutations, and implications for a molecular diagnosis strategy. Circulation. 2003;107(17):2227–32.

[4] Schlossarek S, Mearini G, Carrier L. Cardiac myosin-binding protein C in hypertrophic cardiomyopathy: mechanisms and therapeutic opportunities. J Mol Cell Cardiol. Elsevier Ltd; 2011;50(4):613–20.

[5] Alders M. The 2373insG mutation in the MYBPC3 gene is a founder mutation, which accounts for nearly one-fourth of the HCM cases in the Netherlands. Eur Heart J. 2003;24(20):1848–53.

[6] Moolman JA, Reith S, Uhl K, Bailey S, Gautel M, Jeschke B, et al. A Newly Created Splice Donor Site in Exon 25 of the MyBP-C Gene Is Responsible for Inherited Hypertrophic Cardiomyopathy With Incomplete Disease Penetrance. Circulation. 2000;

[7] Marston S, Copeland O, Jacques A, Livesey K, Tsang V, McKenna WJ, et al. Evidence from human myectomy samples that MYBPC3 mutations cause hypertrophic cardiomyopathy through haploinsufficiency. Circ Res. 2009;105(3):219–22.

[8] Colson B a, Bekyarova T, Fitzsimons DP, Irving TC, Moss RL. Radial displacement of myosin cross-bridges in mouse myocardium due to ablation of myosin binding protein-C. J Mol Biol. 2007;367(1):36–41.

[9] Pohlmann L, Kröger I, Vignier N, Schlossarek S, Krämer E, Coirault C, et al. Cardiac myosin-binding protein C is required for complete relaxation in intact myocytes. Circ Res. 2007;101(9):928–38.

[10] Lecarpentier Y, Vignier N, Oliviero P, Guellich A, Carrier L, Coirault C. Cardiac Myosin-binding protein C modulates the tuning of the molecular motor in the heart. Biophys J. 2008;95(2):720–8.

[11] Witjas-Paalberends ER, Güclü A, Germans T, Knaapen P, Harms HJ, Vermeer AMC, et al. Gene-specific increase in the energetic cost of contraction in hypertrophic cardiomyopathy caused by thick filament mutations. Cardiovasc Res. 2014;103:248–57.

[12] Elliott D a, Braam SR, Koutsis K, Ng ES, Jenny R, Lagerqvist EL, et al. NKX2-5(eGFP/w) hESCs for isolation of human cardiac progenitors and cardiomyocytes. Nat Methods. 2011;8(12):1037–40.

[13] Ng ES, Davis R, Stanley EG, Elefanty AG. A protocol describing the use of a recombinant protein-based, animal product-free medium (APEL) for human embryonic stem cell differentiation as spin embryoid bodies. Nat Protoc. 2008;3(5):768–76.

[14] Birket MJ, Casini S, Kosmidis G, Elliott D a, Gerencser A a, Baartscheer A, et al. PGC-1α and Reactive Oxygen Species Regulate Human Embryonic Stem Cell-Derived Cardiomyocyte Function. Stem Cell Reports. The Authors; 2013;1(6):560–74.

[15] Lan F, Lee AS, Liang P, Sanchez-Freire V, Nguyen PK, Wang L, et al. Abnormal calcium handling properties underlie familial hypertrophic cardiomyopathy pathology in patient-specific induced pluripotent stem cells. Cell Stem Cell. Elsevier Inc.; 2013;12(1):101–13.

[16] Abraham MR. Hypertrophic cardiomyopathy : a heart in need of an energy bar ? 2014;5(August):1–8.

[17] Han L, Li Y, Tchao J, Kaplan AD, Lin B, Li Y, et al. Study familial hypertrophic cardiomyopathy using patient-specific induced pluripotent stem cells. 2014;258–69.

[18] Timmer S a J, Germans T, Brouwer WP, Lubberink M, Van Der Velden J, Wilde A a M, et al. Carriers of the hypertrophic cardiomyopathy MYBPC3 mutation are characterized by reduced myocardial efficiency in the absence of hypertrophy and microvascular dysfunction. Eur J Heart Fail. 2011;13(12):1283–9.

[19] Stoehr A, Neuber C, Baldauf C, Vollert I, Friedrich FW, Flenner F, et al. Automated analysis of contractile force and Ca2+ transients in engineered heart tissue. Am J Physiol Heart Circ Physiol. 2014;306(9):H1353–63.